9-28-2018

Dispersion aerosol indirect effect in turbulent clouds: Laboratory measurements of effective radius

K. K. Chandrakar
Michigan Technological University

Will Cantrell
Michigan Technological University

A. Kostinski
Michigan Technological University

Raymond Shaw
Michigan Technological University

Geophysical Research Letters

RESEARCH LETTER
10.1029/2018GL079194

Dispersion Aerosol Indirect Effect in Turbulent Clouds: Laboratory Measurements of Effective Radius

K. K. Chandrakar[1], W. Cantrell[1], A. B. Kostinski[1], and R. A. Shaw[1]

[1] Atmospheric Sciences Program and Department of Physics, Michigan Technological University, Houghton, MI, USA

Key Points:
- A commonly used, empirical effective radius parameterization is observed under controlled laboratory conditions
- Cloud droplet activation, condensation growth in turbulence, and sedimentation are enough to reproduce stratocumulus observations
- Stochastic condensation growth produces relative size dispersion nearly independent of aerosol concentration for a nonprecipitating cloud

Correspondence to:
R. A. Shaw,
rashaw@mtu.edu

Citation:
Chandrakar, K. K., Cantrell, W., Kostinski, A. B., & Shaw, R. A. (2018). Dispersion aerosol indirect effect in turbulent clouds: Laboratory measurements of effective radius. *Geophysical Research Letters*, *45*. https://doi.org/10.1029/2018GL079194

Received 12 JUN 2018
Accepted 23 SEP 2018
Accepted article online 28 SEP 2018

Abstract Cloud optical properties are determined not only by the number density n_d and mean radius $\bar{r}$ of cloud droplets but also by the shape of the droplet size distribution. The change in cloud optical depth with changing n_d, due to the change in distribution shape, is known as the dispersion effect. Droplet relative dispersion is defined as $d = \sigma_r/\bar{r}$. For the first time, a commonly used effective radius parameterization is tested in a controlled laboratory environment by creating a turbulent cloud. Stochastic condensation growth suggests d independent of n_d for a nonprecipitating cloud, hence nearly zero albedo susceptibility due to the dispersion effect. However, for size-dependent removal, such as in a laboratory cloud or highly clean atmospheric conditions, stochastic condensation produces a weak dispersion effect. The albedo susceptibility due to turbulence broadening has the same sign as the Twomey effect and augments it by order 10%.

Plain Language Summary Clouds cover a large fraction of the Earth and play an important role in determining Earth's climate. Their optical properties, such as how much sunlight they reflect back to space, are determined in part by the number of aerosol particles in the atmosphere. In addition to the mean cloud droplet size, the range of droplet sizes influences cloud optical properties, and that influence is called the dispersion effect. A positive dispersion effect means that an increase in cloud droplet number leads to a more reflective (brighter) cloud. We have carried out experiments in a laboratory cloud chamber to observe how the average size and the range of droplet sizes changes as aerosol concentration is varied. The laboratory chamber creates a turbulent environment. The results show that the the dispersion effect is positive, but small in magnitude. Cloud droplet activation, condensation growth in turbulence, and sedimentation are enough to reproduce stratocumulus observations.

1. Introduction

In a significant way, aerosols affect cloud albedo and lifetime by altering the droplet size distribution. A higher cloud condensation nucleus (CCN) concentration tends to cause a higher concentration of smaller cloud droplets; that, in turn, enhances the cloud reflectivity and also increases the cloud lifetime by suppressing precipitation formation (Albrecht, 1989; Pincus & Baker, 1994; Twomey, 1977, 1974). Collectively, these are referred to as the first and second aerosol indirect effects. Semiempirical parameterization of aerosol and cloud microphysical properties and their influence on cloud optics have been implemented in large-scale models and used to estimate aerosol effects on the radiative balances at a global scale (Brenguier et al., 2000; Feingold & Siebert, 2009; Martin et al., 1994; Seinfeld et al., 2016; Slingo, 1990).

The optical properties of cloud can be expressed through optical depth, single-scattering albedo, and asymmetry parameter. These are functions of two microphysical variables, effective radius of the droplet size distribution $r_e = \overline{r^3}/\overline{r^2}$ and liquid water path (Brenguier et al., 2000; Hansen & Travis, 1974; Stephens, 1978; Slingo, 1989). Coarse-scale atmospheric models and remote sensing retrieval algorithms often depend upon assumptions on how r_e is related to the mean volume radius $r_v = (\overline{r^3})^{1/3}$ and cloud droplet number density n_d (Brenguier et al., 2000; Chen et al., 2007; Han et al., 1998; Platnick & Valero, 1995; Szczodrak et al., 2001). For example, it has been empirically observed that the two are approximately linearly related: $r_v^3 = kr_e^3$ (Martin et al., 1994). This empirical observation is then utilized to parameterize r_e as a function of n_d and other microphysical variables.

The ratio k can be expressed as a function of the relative dispersion of the drop size distribution $d = \sigma_r/\bar{r}$ and its skewness $\mathcal{S}$ (Liu & Daum, 2000; Martin et al., 1994; Pontikis & Hicks, 1992):

$$k = \frac{(1+d^2)^3}{(1+3d^2+Sd^3)^2}, \tag{1}$$

where σ_r is the standard deviation of the droplet size distribution and $\bar{r}$ is the mean droplet radius. The effective radius of a droplet size distribution can then be expressed as (Lu et al., 2007; Martin et al., 1994; Pontikis & Hicks, 1992)

$$r_e \equiv \frac{\int r^3 n(r)\mathrm{d}r}{\int r^2 n(r)\mathrm{d}r} \approx \left[\frac{3L}{4\pi\rho_l n_d k}\right]^{1/3}, \tag{2}$$

where ρ_l is the density of liquid water, n_d is the droplet number concentration, and L is the liquid water content. Equation (2) suggests $r_e \propto n_d^{-1/3}$ as a parameterization (Bower & Choularton, 1992; Pontikis & Hicks, 1992; Slingo, 1990). However, this assumes constant k and liquid water content, L, neither of which need be true.

With equation (2) in mind, we consider how an increase in the aerosol concentration not only increases n_d but also may change the shape of the droplet size distribution. Equation (2) suggests that the cloud optical properties are affected not only by n_d (i.e., the first indirect effect) and liquid water content L but also by the relative dispersion d through k. For example, an increase in n_d enhances cloud albedo directly and also indirectly by decreasing precipitation efficiency and therefore tending to decrease the size dispersion (assuming constant L; Feingold & Siebert, 2009).

Atmospheric observations suggest that the dependence of relative dispersion d on n_d has wide scatter and therefore that the first aerosol-cloud indirect effect (Twomey effect) can be enhanced or suppressed due to changes in the shape of the cloud droplet size distribution (Ackerman et al., 2000; Feingold et al., 1997; Liu & Daum, 2002; Lu & Seinfeld, 2006; Lu et al., 2007, 2012; Peng & Lohmann, 2003; Tas et al., 2012). This can be expressed through the *albedo susceptibility* obtained from the expression of cloud optical depth, $\tau \propto L^{2/3} n_d^{1/3} k^{1/3} h$, where h is the cloud depth (Ackerman et al., 2000; Feingold et al., 1997; Lu & Seinfeld, 2006; Twomey, 1991):

$$\frac{d\ln\tau}{d\ln n_d} = \frac{1}{3} + \frac{2}{3}\frac{d\ln L}{d\ln n_d} + \frac{1}{3}\frac{d\ln k}{d\ln n_d} + \frac{d\ln h}{d\ln n_d}. \tag{3}$$

Here the first term on the right side is the classical effect of droplet number concentration on τ (Twomey effect). The third term $(1/3)(d\ln k/d\ln n_d)$ is known as the dispersion effect and is the focus of this paper. Equation (3) implies that the dispersion (and liquid water content and cloud thickness effects) can enhance or offset the overall aerosol indirect effect beyond the Twomey effect. And yet even the sign of the dispersion effect remains uncertain, with field observations suggesting that it likely depends on CCN spectral width, entrainment, and precipitation development (Feingold et al., 1997; Liu et al., 2006; Yum & Hudson, 2005). Here we consider just the dispersion effect resulting from activation and condensation growth in a turbulent environment (i.e., assuming no collision growth).

Previous studies have generally suggested that condensation growth of cloud droplets leads to narrowing of the droplet size distribution and associated reduction in the relative dispersion, whereas collision-coalescence leads to broadening and increase in d. In recent experimental work, we identified a turbulence-induced size distribution broadening effect that also depends on the CCN concentration (Chandrakar et al., 2016). The results show that as CCN concentration is reduced, the droplet size dispersion σ_r increases dramatically even though droplets only grow by condensation. The droplet size dispersion is thought to be a result of modification of supersaturation fluctuations by cloud droplet growth in a turbulent environment, and a stochastic theory predicts that $d = \sigma_r/\bar{r}$ should be a constant (Chandrakar et al., 2016) or slightly increasing (Chandrakar et al., 2018) depending on assumptions made about droplet removal rate.

In this letter, we explore the dependence of r_e, k and d on CCN concentration using cloud chamber experiments. The experiments are designed such that measurements are made in an environment with steady state turbulence and microphysical properties: droplet growth occurs by condensation and other processes such as entrainment or growth by collision-coalescence can be neglected. These idealizations allow the behavior of r_e, k, and d to be explored in the context of droplet activation, condensation-growth, and sedimentation within a turbulent environment. The experiments therefore provide a way to avoid the complexity that has led to widely varying estimates of the dispersion effect from atmospheric measurements. Furthermore, results can be compared to theoretical predictions for stochastic condensational growth. Our aim is to provide physical insight into aerosol effects on cloud optical properties.

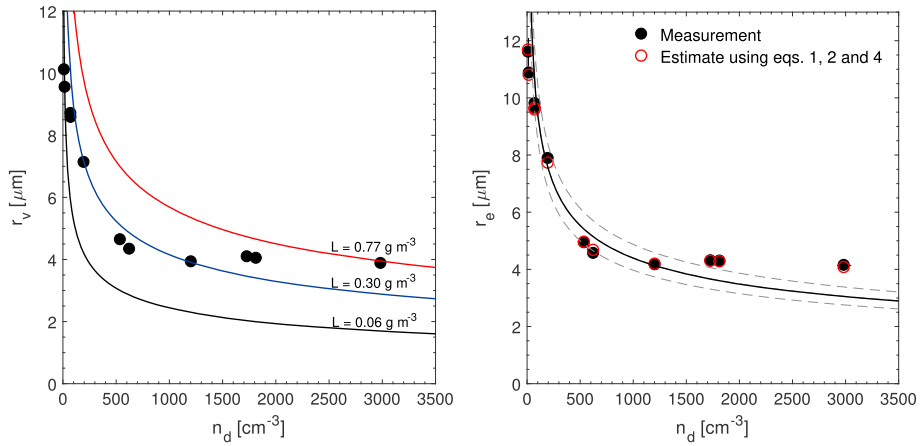

Figure 1. (left) Variation of the mean volume radius for different aerosol injection rates: measurements of mean volume radius (black dots) for different steady state cloud droplet concentrations are shown, and its variation is compared with constant liquid water content contours (solid curves). The constant liquid-water-content L contours $\left(r_v = (3L/4\pi n_d)^{1/3}\right)$ were drawn for the lowest, highest, and intermediate L observed in the measured data set. (right) Variation of the effective radius with the droplet number concentration: steady state values of r_e (black dots) are shown for different n_d (corresponding to different aerosol injection rates). The solid center line is for $L = 0.3$ g/m^3, $k = 0.84$ or $L = 0.22$ g/m^3, $k = 0.62$, and upper and lower dashed lines are for $L = 0.3$ g/m^3 , $k = 0.62$ and $L = 0.22$ g/m^3 , $k = 0.84$ respectively. These values of k are obtained from the fitting in Figure 2. The measurements almost, but do not quite, have a $n_d^{-1/3}$ dependence. Red circles are the theoretical estimates using equations (2), (1), and (4) (please refer to section 3 for detailed discussion).

2. Measurements of Size Dispersion and the Effective Radius Parameter *k*

Experiments are performed in the Michigan Tech Π−chamber by creating a turbulent mixing cloud (Chang et al., 2016). An unstable temperature difference is applied between water saturated top and bottom boundaries of the chamber to create a turbulent supersaturated environment (moist Rayleigh-Bénard convection). In this supersaturated environment, salt aerosols are injected at a constant rate to create cloud droplets. By changing the aerosol injection rates, a range of steady cloud conditions ranging from highly polluted to clean is achieved; that is, in an individual experiment, steady state is achieved through balance between constant aerosol injection and droplet settling. The cloud droplet size distribution and relevant thermodynamic variables are measured for each set of steady state cloud properties. The droplet size measurements were truncated at diameter $\approx$ 5 μm due to lower detectability at smaller sizes. This truncation will influence estimates of n_d and moments of the size distribution, most notably for high aerosol concentrations (Chandrakar et al., 2018). Quantities such as r_e that depend on high moments such as $\overline{r^2}$ and $\overline{r^3}$ are not strongly influenced because of their dependence on the large-size tail of the distribution. Fitting of the measurements with a gamma distribution and computing changes in r_e and k confirms that variation with n_d only change slightly. The details of the experiments and the data set that are used in this paper, as well as an overview of the stochastic condensation growth theory are provided by Chandrakar et al. (2018). Here we focus on analysis of those results in the context of r_e, k, and implications for the dispersion effect via equations (1)–(3).

Steady state experiments in the cloud chamber with different input values of CCN result in observed dependence of r_v and r_e on n_d as shown in Figure 1. The left panel shows the decrease in r_v with n_d in response to an increase in the aerosol injection rate, along with contours of constant liquid water content L. It varies from 0.06 to 0.77 g/m^3 with increasing aerosol injection rate, which is a result of the decreased droplet settling speed and associated increase in droplet lifetime. The r_e corresponding to these cases is shown in the right panel of the figure, along with curves obtained from equation (2) assuming constant L and k. Deviation of the data points from the curves implies departure from the simple $r_e \propto n_d^{-1/3}$ parameterization (Bower & Choularton, 1992; Pontikis & Hicks, 1992; Slingo, 1990). Moreover, the solid and dashed lines in the right panel of the figure demonstrate that the assumption of a constant parameter k does not fully describe the data. As can be seen, different data points follow different constant k lines, and the L and k combination for a data point is not unique.

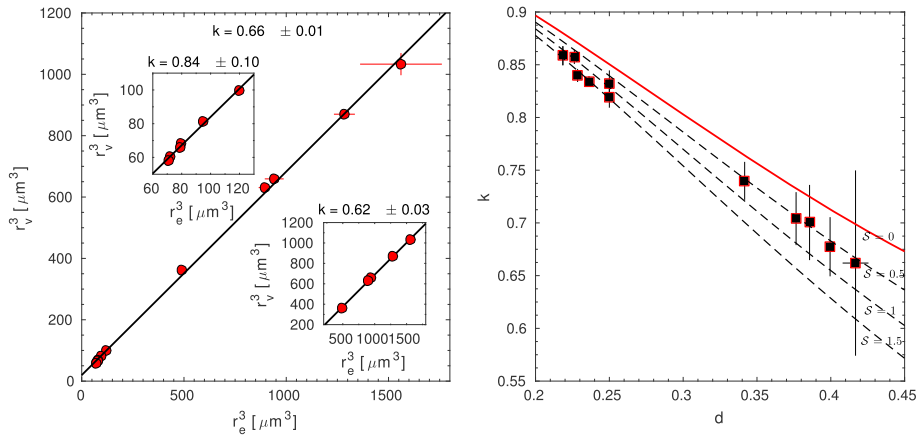

Figure 2. (left) The nearly (not exactly) linear relationship between r_v^3 and r_e^3: experimental results (red dots) are fitted with a linear curve (black line), resulting in $k = 0.66$. Inset figures reveal that the nearly linear behavior of r_v^3 versus r_e^3 is not precisely true; rather, the slope k is different for the clean (lower right) and polluted (upper left) regimes. (right) Variation of the parameter $k = r_v^3/r_e^3$ with the relative dispersion (black square) and its comparison with the estimates (open red square) from equation (1). The solid red line shows equation (1) for zero skewness. Dashed lines are for three skewness values, showing that $S \approx 0.5$ to 1.5. For comparison, Martin et al. (1994) observed $k = 0.67$ and $k = 0.80$ for continental and maritime stratocumulus cloud cases, respectively.

These results suggest that insight can be obtained into the linearity assumption $r_v^3 = kr_e^3$ using steady state cloud data from the Π-chamber. The left panel of Figure 2 shows r_v^3 and r_e^3 for a range of different aerosol injection rates, with constant turbulence forcing in the cloud chamber. Each of the data points in the figure corresponds to a steady state droplet size distribution (averaged over a time scale $\sim \mathcal{O}$, 200 min) for different aerosol injection rates. The figure confirms an approximately linear relationship between the cubic mean volume radius (r_v^3) and cubic effective radius (r_e^3). The slope of the best fit line to the data is $k = 0.66$, which is close to the range of k (0.67–0.8) observed in the atmosphere (Martin et al., 1994). However, closer examination reveals that k does vary, for example, with aerosol loading: the two insets show linear fits for just the polluted cloud (upper left) and clean cloud (lower right), resulting in k varying from 0.62 to 0.84. The results are numerically similar but opposite from the in situ observations of Martin et al. (1994), which resulted in $k = 0.67 \pm 0.07$ for continental stratocumulus clouds and $k = 0.80 \pm 0.07$ for maritime stratocumulus clouds.

In the right panel of Figure 2, the parameter k is calculated directly from each steady state cloud droplet size distribution using equation (1). The measurements (black squares) show a monotonic dependence of k on relative dispersion d, decreasing with increasing d as expected from equation (1). The experimental data points lie away from the theoretical curve with $\mathcal{S} = 0$ (red line), showing the importance of the skewness of the distributions as expressed in equation (1). Skewness is observed to range from $S \approx 0.5$ to 1.5. The primary contribution to the observed variation in k is from d, with skewness making a smaller contribution. Martin et al. (1994) and Liu and Daum (2000) showed that the effect of skewness in r_e parameterization is significant when d is large. In the current study, the effect of skewness is explored without assuming any distribution shape. But taking a gamma distribution as an example, the relative dispersion d and the skewness S are both proportional to $a^{-1/2}$, where a is the unitless shape parameter, and are independent of the scale parameter. Therefore, a gamma distribution is only able to describe the current observations if a is taken to be a function of d, and therefore of n_d. Finally, as a consistency check, calculations of k from equation (1) are made (red squares). The results adequately follow the values from a direct calculation, confirming that higher moments do not contribute and equation (1) is a reasonable representation of the dependence of k on d.

The change in d observed in the measurements is a direct consequence of varying the CCN concentration and the resulting cloud droplet concentration. In Figure 3 we show the dependence of k on n_d for each observed, steady state cloud droplet size distribution (black squares). The measurements show that k is a weak function of droplet number concentration n_d, consistent with the original findings of Martin et al. (1994). The parameter k is observed to increase nearly linearly with increasing n_d in relatively clean clouds, similar to the observations from marine stratocumulus clouds by Lu et al. (2007). This is in contrast to Martin et al. (1994), who observed larger k for maritime compared to continental stratocumulus clouds, and therefore an

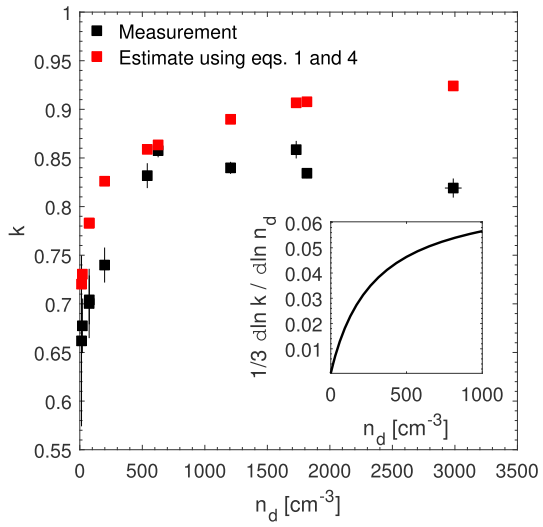

Figure 3. Variation of the parameter k with droplet number concentration n_d: steady state values of k (black squares) obtained for the n_d that occur for different aerosol injection rates. Inset figure: An estimate of the dispersion effect, as defined in equation (3). The albedo susceptibility due to droplet size dispersion is obtained using a power law fit of the k versus n_d measurements for the range $n_d < 10^3$ cm^{-3} (since k is nearly constant after that point). The magnitude of the dispersion effect in the inset is to be compared to the Twomey effect 1/3 defined in equation (3). Calculated k values using equations (1) and (4) are shown as red squares.

opposite sign of the dispersion effect. Interestingly, the data seem to suggest two regimes: a nearly linear increase in k with increasing n_d under low-n_d conditions, and a nearly constant k for relatively large n_d. However, the variation of k with n_d is modest, changing by only 22% for a factor of nearly 200 increase in the droplet concentration. The inset in Figure 3 shows an estimate of the magnitude of the dispersion effect $(1/3)d\ln k/d\ln n_d$ for the low-n_d regime, using a power law fit to the data. The dispersion effect is observed to be of order 10% of the Twomey effect value 1/3.

3. Dispersion Effect and Atmospheric Implications

We now attempt to interpret the dependence of k on n_d using the stochastic condensation approach outlined by Chandrakar et al. (2016). The approach can be qualitatively summarized as follows: supersaturation is assumed to vary randomly due to mixing, entrainment, fluctuations in vertical velocity, or variations in cloud microphysical properties (Desai et al., 2018). Given s_o as the expected value of the mean supersaturation without any cloud droplet formation (i.e., it is the expected value of the supersaturation that would exist for the same forcing if there were no water vapor loss due to cloud formation), the mean supersaturation in the presence of cloud, $\bar{s}$, is given by $\bar{s} = s_0/(1 + \tau_t/\tau_c)$. Here τ_t/τ_c, is the ratio of the turbulence correlation time scale, τ_t, and the phase relaxation time, $\tau_c = (4\pi D'_v \bar{r} n_d)^{-1}$, where D'_v is the water vapor diffusion coefficient modified to account for heat conduction (Kumar et al., 2013; Rogers & Yau, 1989). The τ_c corresponds to the characteristic time for adjustment of supersaturation resulting from droplet growth by condensation. Chandrakar et al. (2016) showed that the width of a cloud droplet size distribution becomes much broader for small τ_t/τ_c, corresponding to relatively low CCN and n_d, in what can be termed the slow microphysics/fast turbulence regime. The data set used in this study spans a τ_t/τ_c range of 0.44 - 40.23, with the $\tau_t/\tau_c = 1$ transition occurring between the $n_d = 75.9$ and 198.4 cm^{-3} data points. Thus, the observed saturation of k with increasing n_d in Figure 3 corresponds to clouds in the $\tau_t/\tau_c > 1$ regime, that is, to fast microphysics and slow turbulence.

Equation (1) suggests that the parameter k depends mainly on the relative dispersion. As just discussed, however, the relative dispersion resulting from stochastic condensation depends on the aerosol loading and corresponding cloud droplet concentration. Using the central result of Chandrakar et al. (2016) for σ_{r^2} and the fact that $\overline{r^2} \propto \bar{s}t$ (Rogers & Yau, 1989), the relative dispersion for r^2 can be written as

$$d_a = \frac{\sigma_{r^2}}{\overline{r^2}} \propto \left(\frac{\sigma_{s_0}}{s_0}\right)\left(\frac{\tau_t}{t}\right)^{1/2}. \tag{4}$$

We can take t as the average droplet lifetime τ_l. This is an interesting result because it suggests that d_a has no explicit dependence on n_d. For the Π chamber results shown in Figures 1 and 2, however, there is at least a modest change in d_a as aerosol injection rate and n_d are increased. It is indeed reasonable to expect that the droplet lifetime depends on the rate of droplet growth and therefore the mean supersaturation. Following Yang et al. (2014), that dependence is $\tau_l \propto \bar{s}^{-1/2}$, and as discussed earlier, mean supersaturation has a dependence on the phase relaxation time $\bar{s} = s_0/(1 + \tau_t/\tau_c)$. Consequently, $\tau_l \propto \left(s_o/(4\pi D'_v n_d \bar{r}\tau_t)\right)^{-1/2}$, where the expression for the phase relaxation time τ_c has been used. The implication is that d_a should have a dependence on the product $n_d\bar{r}$ since other factors such as τ_t are held constant during the experiments. Taken together, these results lead to the following scaling for relative dispersion in the Π chamber: $d_a \propto (\sigma_{s_0}/s_o)\left(1 + 4\pi D'_v \tau_t \bar{r} n_d\right)^{-1/4}$. A more complete derivation is given by Chandrakar et al. (2018), but this simpler approach is adequate for our purposes because all other factors in the final expression are constant in the experiments except $\bar{r}$ and n_d.

Figures 1 (right panel) and 3 show estimates of r_e and k using equations 1 and 4. To compare, we make the approximation $d_a \approx 2d$. The individual points are based on the measured values of $\bar{r}$ and n_d, and use the same,

constant proportionality factor for equation (4), obtained through best fit of the measured droplet size statistics. Equation (4) with the functional dependence of droplet lifetime reasonably captures the behavior of the experimental data points. Thus, we conclude that the weak observed dispersion effect in the cloud chamber experiments is fundamentally a result of the droplet size dependence of the removal rate. The stochastic condensation process itself suggests constant k, assuming constant environmental conditions leading to supersaturation variability, and therefore zero dispersion effect; the positive and small dispersion effect results from larger droplets being removed more rapidly than small droplets.

Using the expression for droplet relative dispersion, equation (4) and the definition of k, equation (1), the albedo susceptibility due to the dispersion effect can be obtained. It is relevant to droplet condensation growth in the presence of turbulent fluctuations of water vapor concentration and temperature, and in the absence of collision-coalescence. It also is based on the assumption that droplet removal is due to gravitational sedimentation, as occurs in the cloud chamber. This scenario has atmospheric relevance as well, for clouds in extremely clean (low CCN concentration) environments where cloud droplets growth solely by condensation are removed as precipitation (Mauritsen et al., 2011). The dependence of sedimentation rate on droplet radius, along with the dependence of mean radius on n_d, leads to a dependence of d and k on n_d. The resulting albedo susceptibility due to the dispersion effect has a positive sign. We obtain a quantitative estimate of the dispersion effect by fitting a smooth function to the observations of k in Figure 3, and then taking its derivative. The result is shown in the inset to Figure 3 for the range $n_d < 10^3$ cm^{-3}. As expected from the n_d dependence of droplet lifetime in equation (4), it increases with an increase in n_d. Its magnitude is small in comparison to the Twomey effect, with a maximum value around 15%. That is a direct result of the relative dispersion having a weak dependence on droplet concentration; that is, d_a changes by a factor of 2 with a $\approx$ 200 times increase in n_d.

As can be inferred from equation (4), the relative dispersion of droplet size distribution is independent of n_d if droplet removal is not size dependent. It just depends on thermodynamic and turbulence properties, and the cloud droplet lifetime. If there is no size-dependent droplet removal (like, sedimentation in case of the cloud chamber) and activation, that is, a closed parcel, the stochastic theory suggests dependence of the size distribution width on aerosol concentration. However, the relative dispersion at a fixed growth time t turns out to be independent of aerosol number. This statement is based purely on stochastic condensation without any influence of other factors, such as the activation-based dispersion effect for different aerosol-cloud interaction regimes (Chen et al., 2016; Liu et al., 2006; Yum & Hudson, 2005). Consequently, it implies that the albedo susceptibility due to dispersion effect based on stochastic condensation alone will be zero for a cloud with no size-dependent removal. This condition is nearly true for nondrizzling stratocumulus clouds where size-dependent removal processes (such as gravitational removal and droplet collision-coalescence) are not active. However, more subtle effects are possible: for example, a change in the aerosol population might indirectly affect the dispersion effect by suppressing the onset of droplet collision process and enhancing the cloud droplet lifetime. Observations in the atmosphere indeed show differing relative dispersion trends with aerosol concentration: some suggest an increase in relative dispersion (negative dispersion effect; Liu & Daum, 2002; Martin et al., 1994; Miles et al., 2000; Pawlowska et al., 2006; Peng & Lohmann, 2003), some a decreasing relative dispersion (positive dispersion effect; ; Lu et al., 2007, 2012, 2013; Miles et al., 2000), and some a relatively constant or unclear trend (Arabas et al., 2009; Lu et al., 2008; Miles et al., 2000; Tas et al., 2015; Zhao et al., 2006) with aerosol concentration. These observation of nonconstant behavior of relative dispersion might result from a variety of processes, like onset of collision-coalescence, dynamic effects (entrainment and mixing), or predominance of an early growth stage in which the initial aerosol distribution influences the size dispersion (Feingold et al., 1997; Lu et al., 2013; Peng et al., 2007; Tas et al., 2012; Yum & Hudson, 2005). Consequently, one needs to be cautious in comparing the dispersion effect from clouds having different thermodynamic conditions, different stages of development, or the different regions or stages where entrainment and mixing dominate the overall growth process (Schmeissner et al., 2015).

4. Discussion and Conclusions

Physically based representations (i.e., parameterizations) of aerosol-cloud microphysical processes are needed for remote sensing retrieval methods and for coarse-resolution atmospheric models, including those used for climate studies. Much effort has been made to develop empirical microphysical parameterizations using field measurements of clouds. However, variability in the atmospheric cloud conditions and complex feedbacks make it attractive to test some of the parameterizations in a controlled laboratory environment.

Therefore, we have generated turbulent cloud conditions in an isolated laboratory chamber and have tested some commonly used expressions using the resulting statistically steady cloud microphysical data set. This approach allows us to have well-characterized thermodynamic, turbulence, and microphysical conditions, and long enough, steady data sets for critical scrutiny of these parameterizations. Furthermore, the experiments allow certain physical processes, namely, condensation growth of cloud droplets in a turbulent environment, to be isolated from other processes, including dry-air entrainment and collision-coalescence. We address the influence of condensation growth in turbulence, modulated by aerosol concentration, on calculated cloud radiative properties; specifically, this study is focused on the effective radius and the dispersion aerosol-indirect effect. Observations are interpreted in the context of a theoretical description of cloud droplet growth in a turbulent environment. A positive, weak albedo susceptibility is observed for the cloud chamber conditions, resulting from the droplet size dependence of the removal rate. It is hoped that this work will help in establishing a physical foundation for further development of microphysical parameterization for atmospheric clouds.

A commonly used parameterization of the effective radius ($r_v^3 = kr_e^3$) developed based on measurements of the stratocumulus clouds is observed to also hold for turbulent clouds generated in the Π-Chamber. The measurements of slope parameter k are consistent with the range of values from stratocumulus cloud measurements (Lu et al., 2007; Martin et al., 1994). The validity of this linear fit over a large range of n_d suggests that the parameter k is weakly changing over this range. Pioneering work has shown that the parameter k is a function of the relative dispersion and skewness of the cloud droplet size distribution (Liu & Daum, 2000; Martin et al., 1994; Pontikis & Hicks, 1992). Given the dependence of k on the width and skewness of the droplet size distribution, we expect from prior work there will be a link to aerosol (CCN) concentration when droplet growth occurs in a turbulent environment (Chandrakar et al., 2016, 2018; Desai et al., 2018), and indeed, a positive, albeit weak dispersion effect is observed.

Martin et al. (1994) suggested that measurement data points from stratocumulus and cumulus clouds sometimes deviate strongly from a linear $r_v^3 = kr_e^3$ relation. They interpreted this deviation as a result of entrainment of cloud-free air from cloud top and edges. This indicates the importance of turbulent flow conditions and demands further investigation of the influence of turbulence and entrainment. The results presented here also suggest an influence of turbulent fluctuations on the microphysics and related cloud optical parameters. A particularly intriguing possibility arises if the main droplet removal mechanism is entrainment and subsequent evaporation. If the dilution and removal of droplets through evaporation takes place via homogeneous mixing, then there is a preference to remove smaller droplets earlier, which would tend to result in a negative dispersion effect. In contrast, if the removal of droplets through evaporation takes place via inhomogeneous mixing, then all droplets have equal probability of removal, resulting in zero dispersion effect.

Acknowledgments
We thank D. Ciochetto and G. Kinney for assistance with the experiments. This work was supported by National Science Foundation grants AGS-1754244 and AGS-1639868 and by NASA Headquarters under the NASA Earth and Space Science Fellowship Program — Grant 80NSSC17K0449. Data from the experiments are available at https://digitalcommons.mtu.edu/physics-fp/137/.

References

Ackerman, A. S., Toon, O. B., Taylor, J. P., Johnson, D. W., Hobbs, P. V., & Ferek, R. J. (2000). Effects of aerosols on cloud albedo: Evaluation of Twomey's parameterization of cloud susceptibility using measurements of ship tracks. *Journal of the Atmospheric Sciences*, *57*(16), 2684–2695. https://doi.org/10.1175/1520-0469(2000)057<2684:EOAOCA>2.0.CO;2

Albrecht, B. A. (1989). Aerosols, cloud microphysics, and fractional cloudiness. *Science*, *245*(4923), 1227–1230.

Arabas, S., Pawlowska, H., & Grabowski, W. W. (2009). Effective radius and droplet spectral width from in-situ aircraft observations in trade-wind cumuli during RICO. *Geophysical Research Letters*, *36*, L11803. https://doi.org/10.1029/2009GL038257

Bower, K., & Choularton, T. (1992). A parameterisation of the effective radius of ice free clouds for use in global climate models. *Atmospheric Research*, *27*(4), 305–339.

Brenguier, J.-L., Pawlowska, H., Schüller, L., Preusker, R., Fischer, J., & Fouquart, Y. (2000). Radiative properties of boundary layer clouds: Droplet effective radius versus number concentration. *Journal of the Atmospheric Sciences*, *57*(6), 803–821.

Chandrakar, K., Cantrell, W., Chang, K., Ciochetto, D., Niedermeier, D., Ovchinnikov, M., et al. (2016). Aerosol indirect effect from turbulence-induced broadening of cloud-droplet size distributions. *Proceedings of the National Academy of Sciences of the United States of America*, *113*, 14,243–14,248.

Chandrakar, K., Cantrell, W., & Shaw, R. (2018). Influence of turbulent fluctuations on cloud droplet size dispersion and aerosol indirect effects. *Journal of the Atmospheric Sciences*, *75*(9), 3191–3209.

Chang, K., Bench, J., Brege, M., Cantrell, W., Chandrakar, K., Ciochetto, D., et al. (2016). A laboratory facility to study gas-aerosol-cloud interactions in a turbulent environment: The Π Chamber. *Bulletin of the American Meteorological Society*, *97*, 2343–2358.

Chen, R., Chang, F.-L., Li, Z., Ferraro, R., & Weng, F. (2007). Impact of the vertical variation of cloud droplet size on the estimation of cloud liquid water path and rain detection. *Journal of the Atmospheric Sciences*, *64*(11), 3843–3853. https://doi.org/10.1175/2007JAS2126.1

Chen, J., Liu, Y., Zhang, M., & Peng, Y. (2016). New understanding and quantification of the regime dependence of aerosol-cloud interaction for studying aerosol indirect effects. *Geophysical Research Letters*, *43*, 1780–1787. https://doi.org/10.1002/2016GL067683

Desai, N., Chandrakar, K. K., Chang, K., Cantrell, W., & Shaw, R. A. (2018). Influence of microphysical variability on stochastic condensation in a turbulent laboratory cloud. *Journal of the Atmospheric Sciences*, *75*(1), 189–201. https://doi.org/10.1175/JAS-D-17-0158.1

Feingold, G., Boers, R., Stevens, B., & Cotton, W. R. (1997). A modeling study of the effect of drizzle on cloud optical depth and susceptibility. *Journal of Geophysical Research*, *102*(D12), 13,527–13,534.

Feingold, G., & Siebert, H. (2009). *Cloud-aerosol interactions from the micro to the cloud scale* (pp. 319–338). Cambridge, MA: MIT Press..
Han, Q., Rossow, W. B., Chou, J., & Welch, R. M. (1998). Global survey of the relationships of cloud albedo and liquid water path with droplet size using ISCCP. *Journal of Climate*, *11*(7), 1516–1528.
Hansen, J. E., & Travis, L. D. (1974). Light scattering in planetary atmospheres. *Space Science Reviews*, *16*(4), 527–610.
Kumar, B., Schumacher, J., & Shaw, R. A. (2013). Cloud microphysical effects of turbulent mixing and entrainment. *Theoretical and Computational Fluid Dynamics*, *27*(3-4), 361–376.
Liu, Y., & Daum, P. H. (2000). Spectral dispersion of cloud droplet size distributions and the parameterization of cloud droplet effective radius. *Geophysical Research Letters*, *27*(13), 1903–1906.
Liu, Y., & Daum, P. H. (2002). Anthropogenic aerosols: Indirect warming effect from dispersion forcing. *Nature*, *419*(6907), 580–581.
Liu, Y., Daum, P. H., & Yum, S. S. (2006). Analytical expression for the relative dispersion of the cloud droplet size distribution. *Geophysical Research Letters*, *33*, L02810. https://doi.org/10.1029/2005GL024052
Lu, M.-L., Conant, W. C., Jonsson, H. H., Varutbangkul, V., Flagan, R. C., & Seinfeld, J. H. (2007). The Marine Stratus/Stratocumulus Experiment (MASE): Aerosol-cloud relationships in marine stratocumulus. *Journal of Geophysical Research*, *112*, D10209. https://doi.org/10.1029/2009JD012774
Lu, M., Feingold, G., Jonsson, H. H., Chuang, P. Y., Gates, H., Flagan, R. C., & Seinfeld, J. H. (2008). Aerosol-cloud relationships in continental shallow cumulus. *Journal of Geophysical Research*, *113*, D15201. https://doi.org/10.1029/2007JD009354
Lu, C., Liu, Y., Niu, S., & Vogelmann, A. M. (2012). Observed impacts of vertical velocity on cloud microphysics and implications for aerosol indirect effects. *Geophysical Research Letters*, *39*, L21808. https://doi.org/10.1029/2012GL053599
Lu, C., Niu, S., Liu, Y., & Vogelmann, A. M. (2013). Empirical relationship between entrainment rate and microphysics in cumulus clouds. *Geophysical Research Letters*, *40*, 2333–2338. https://doi.org/10.1002/grl.50445
Lu, M.-L., & Seinfeld, J. H. (2006). Effect of aerosol number concentration on cloud droplet dispersion: A large-eddy simulation study and implications for aerosol indirect forcing. *Journal of Geophysical Research*, *111*, D02207. https://doi.org/10.1029/2005JD006419
Martin, G., Johnson, D., & Spice, A. (1994). The measurement and parameterization of effective radius of droplets in warm stratocumulus clouds. *Journal of the Atmospheric Sciences*, *51*(13), 1823–1842.
Mauritsen, T., Sedlar, J., Tjernström, M., Leck, C., Martin, M., Shupe, M., et al. (2011). An arctic CCN-limited cloud-aerosol regime. *Atmospheric Chemistry and Physics*, *11*(1), 165–173. https://doi.org/10.5194/acp-11-165-2011
Miles, N. L., Verlinde, J., & Clothiaux, E. E. (2000). Cloud droplet size distributions in low-level stratiform clouds. *Journal of the Atmospheric Sciences*, *57*(2), 295–311. https://doi.org/10.1175/1520-0469(2000)057<0295:CDSDIL>2.0.CO;2
Pawlowska, H., Grabowski, W. W., & Brenguier, J.-L. (2006). Observations of the width of cloud droplet spectra in stratocumulus. *Geophysical Research Letters*, *33*, L19810. https://doi.org/10.1029/2006GL026841
Peng, Y., & Lohmann, U. (2003). Sensitivity study of the spectral dispersion of the cloud droplet size distribution on the indirect aerosol effect. *Geophysical Research Letters*, *30*(10), 1507. https://doi.org/10.1029/2003GL017192
Peng, Y., Lohmann, U., Leaitch, R., & Kulmala, M. (2007). An investigation into the aerosol dispersion effect through the activation process in marine stratus clouds. *Journal of Geophysical Research*, *112*, D11117. https://doi.org/10.1029/2006JD007401
Pincus, R., & Baker, M. (1994). Effect of precipitation on the albedo susceptibility of clouds in the marine boundary layer. *Nature*, *372*(6503), 250–252.
Platnick, S., & Valero, F. P. (1995). A validation of a satellite cloud retrieval during ASTEX. *Journal of the Atmospheric Sciences*, *52*(16), 2985–3001.
Pontikis, C., & Hicks, E. (1992). Contribution to the cloud droplet effective radius parameterization. *Geophysical Research Letters*, *19*(22), 2227–2230.
Rogers, R., & Yau, M. (1989). *A short course in cloud physics*. Oxford, UK: Butterworth-Heinemann.
Schmeissner, T., Shaw, R., Ditas, J., Stratmann, F., Wendisch, M., & Siebert, H. (2015). Turbulent mixing in shallow trade wind cumuli: Dependence on cloud life cycle. *Journal of the Atmospheric Sciences*, *72*(4), 1447–1465.
Seinfeld, J. H., Bretherton, C., Carslaw, K. S., Coe, H., DeMott, P. J., Dunlea, E. J., et al. (2016). Improving our fundamental understanding of the role of aerosol-cloud interactions in the climate system. *Proceedings of the National Academy of Sciences of the United States of America*, *113*(21), 5781–5790.
Slingo, A. (1989). A GCM parameterization for the shortwave radiative properties of water clouds. *Journal of the Atmospheric Sciences*, *46*(10), 1419–1427.
Slingo, A. (1990). Sensitivity of the Earth's radiation budget to changes in low clouds. *Nature*, *343*(6253), 49–51.
Stephens, G. L. (1978). Radiation profiles in extended water clouds. II: Parameterization schemes. *Journal of the Atmospheric Sciences*, *35*(11), 2123–2132.
Szczodrak, M., Austin, P. H., & Krummel, P. (2001). Variability of optical depth and effective radius in marine stratocumulus clouds. *Journal of the Atmospheric Sciences*, *58*, 2912–2926.
Tas, E., Koren, I., & Altaratz, O. (2012). On the sensitivity of droplet size relative dispersion to warm cumulus cloud evolution. *Geophysical Research Letters*, *39*, L13807. https://doi.org/10.1029/2012GL052157
Tas, E., Teller, A., Altaratz, O., Axisa, D., Bruintjes, R., Levin, Z., & Koren, I. (2015). The relative dispersion of cloud droplets: Its robustness with respect to key cloud properties. *Atmospheric Chemistry and Physics*, *15*(4), 2009–2017.
Twomey, S. (1974). Pollution and the planetary albedo. *Atmospheric Environment (1967)*, *8*(12), 1251–1256.
Twomey, S. (1977). The influence of pollution on the shortwave albedo of clouds. *Journal of the Atmospheric Sciences*, *34*(7), 1149–1152.
Twomey, S. (1991). Aerosols, clouds and radiation. *Atmospheric Environment*, *25*, 2435–2442.
Yang, F., Ovchinnikov, M., & Shaw, R. A. (2014). Microphysical consequences of the spatial distribution of ice nucleation in mixed-phase stratiform clouds. *Geophysical Research Letters*, *41*, 5280–5287. https://doi.org/10.1002/2014GL060657
Yum, S. S., & Hudson, J. G. (2005). Adiabatic predictions and observations of cloud droplet spectral broadness. *Atmospheric Research*, *73*(3-4), 203–223.
Zhao, C., Tie, X., Brasseur, G., Noone, K. J., Nakajima, T., Zhang, Q., et al. (2006). Aircraft measurements of cloud droplet spectral dispersion and implications for indirect aerosol radiative forcing. *Geophysical Research Letters*, *33*, L16809. https://doi.org/10.1029/2006GL026653